Title: Glial activation precedes alpha-synuclein pathology in a mouse model of Parkinson's disease.

Authors: Maria Izco[1*] PhD, F Javier Blesa[2] PhD, Guglielmo Verona[3] PhD, J Mark Cooper[4] PhD, Lydia Alvarez-Erviti[1*] PhD

Affiliations:

[1] Laboratory of Molecular Neurobiology, Center for Biomedical Research of La Rioja (CIBIR), Piqueras 98, 3th floor, 26006, Logroño, Spain.

[2] HM CINAC, Hospital Universitario HM Puerta del Sur, Av. Carlos V, 70, 28938 Móstoles, Madrid, Spain.

[3] Wolfson Drug Discovery Unit, Centre for Amyloidosis and Acute Phase Proteins, UCL, Gower Street, London, United Kingdom

[4] Department of Clinical Neuroscience, Institute of Neurology, UCL, Gower Street, London, UK.

* **Corresponding authors**: Lydia Alvarez-Erviti (laerviti@riojasalud.es)
Maria Izco (mizco@riojasalud.es)
Laboratory of Molecular Neurobiology
Center for Biomedical Research of La Rioja (CIBIR)
Piqueras 98, 3th floor, 26006 Logroño (La Rioja)
Telephone: +34 941 278 791

Declarations of interest: none

Total number of pages: 34

Total number of figures: 5

Total number of tables: 1

Abstract

Neuroinflammation is increasingly recognized as an important feature in the pathogenesis of Parkinson's disease (PD). However, it remains unclear whether neuroinflammation contributes to nigral degeneration in PD or is merely a secondary marker of neurodegeneration. We aimed to investigate the temporal relationship between synucleopathy, neuroinflammation and nigrostriatal degeneration in a mouse model of PD. Mice received unilateral intrastriatal injection of alpha-synuclein pre-formed fibrils, alpha-synuclein monomer or vehicle and were sacrificed at 15, 30 and 90 days post-injection. Intrastriatal inoculation of alpha-synuclein fibrils led to significant alpha-synuclein aggregation in the substantia nigra peaking at 30 days after injection while the significant increase in Iba-1 cells, GFAP cells and IL-1β expression peaked earlier at 15 days. At 90 days, the striatal dopaminergic denervation was associated with astroglial activation. Alpha-synuclein monomer did not result in long-term glia activation or increase in inflammatory markers. The spread of alpha-synuclein aggregates into the cortex was not associated with any changes to neuroinflammatory markers. Our results demonstrate that in the substantia nigra glial activation is an early event that precedes alpha-synuclein inclusion formation, suggesting neuroinflammation could play an important early role in the pathogenesis of PD.

Keywords: Parkinson's disease, mouse model, alpha-synuclein, neuroinflammation, microglia, astrocytes

Main text

Introduction

Parkinson's disease (PD) is the second most prevalent neurodegenerative disorder worldwide but effective disease modifying treatments are still awaited (Olanow et al., 2017). PD is characterized neuropathologically by the presence of intraneuronal Lewy bodies (LB) containing misfolded alpha-synuclein (α-syn), and the predominant loss of dopamine (DA) neurons in the substantia nigra pars compacta (SNpc) leading to bradykinesia, tremor and postural instability (Fearnley et al., 1991).

While the primary cause of PD in the majority of the patients remains unknown, the rare genetic causes of PD have helped support several possible pathogenic mechanisms (Greenamyre et al., 2004; Lin and Beal, 2006; Schapira, 2006; Dick, 2012; Ebrahimi-Fakhari et al., 2012). The role of neuroinflammation and glial cell activation in PD has gained increased attention in recent years and are recognized as crucial features of PD pathogenesis, but it is unclear if they are drivers of disease progression and the selective loss of DA neurons. Genome wide association studies have found that polymorphisms in the HLA-DR (human MHCII) loci are associated with late-onset PD (Hamza et al., 2010). Indeed, pro-inflammatory cytokines are significantly elevated not only in plasma and cerebrospinal fluid (CSF) of PD patients but also in postmortem brain tissue (Mogi et al., 1994; Blum-Degen et al., 1995; Lindqvist et al., 2013). Animal studies have demonstrated progressive dopaminergic cell death and motor disabilities induced by sustained expression of different pro-inflammatory cytokines in the SNpc, which support the involvement of these pro-inflammatory cytokines in PD pathogenesis (Ferrari et al., 2006; De Lella-Ezcurra et al., 2010), and critically non-steroidal anti-inflammatory drugs have been shown to lower the risk of developing PD (Gagne et al., 2010; Manthripragada et al., 2011).

In the central nervous system (CNS), immune responses are mainly mediated by microglia and astrocytes. Microglial cells are the resident innate immune cells of the brain, which,

have a role in monitoring the brain for damage and invading pathogens. Upon changes in their surrounding environment, microglial cells activate, change their morphology ranging from hyper-ramified, hypertrophic or ameboid morphology and secrete different cytokines with functional consequences in the CNS. Since the first report showing activation of microglia in the SNpc of PD postmortem brains (McGeer et al., 1988), numerous studies have been published describing microglial changes in patients as well as in genetic and neurotoxic-based animal models of PD (McGeer et al., 2008; Long-Smith et al., 2009; Halliday and Stevens, 2011). Furthermore, the post-mortem data have been confirmed by in vivo positron emission tomography (PET) studies in PD patients, which also show a pronounced activation of microglia in the basal ganglia of PD brains in early and late stages of the disease (Gerhard et al., 2006; Bartels et al., 2010). Apart from microglial activation, numerous studies shows that astrocytes are activated in PD. Reactive astrogliosis characterized by the increased expression of glial fibrillary acidic protein (GFAP) have been reported in experimental PD animal models (Lee et al., 2010; Barcia et al., 2011) and in affected brain areas in PD patients (Yamada et al., 1992).

While these studies support a role for neuroinflammation in PD pathogenesis, its cause and temporal involvement has not yet been resolved. It remains unclear whether neuroinflammation contributes to nigral degeneration and disease progression in PD or is merely a secondary consequence of cell death. Recently, Luk et al. developed a progressive mouse model of PD based on the intrastriatal injection of alpha-synuclein pre-formed fibrils (α-syn PFF) into young wild type (WT) mice that recapitulates the time-dependent accumulation and propagation of LB-like α-syn pathology, death of nigrostriatal DA neurons and impairment of motor coordination (Luk et al., 2012). We have used this model to explore the temporal relationship between synucleinopathy, neuroinflammation and nigrostriatal degeneration. We observed microglia and astrocyte activation in SNpc prior to the development of α-syn pathology, suggesting that neuroinflammation precedes and potentially could drive dopaminergic dysfunction. These results implicate microglia and

astrocytes as important early mediators of PD pathogenesis and represent potential targets for early therapeutic interventions.

Materials and methods

- Preparation of mouse wild-type α-syn PFFs

Recombinant mouse wild-type α-syn was dissolved in sterile PBS (pH 7.4) and the concentration was carefully adjusted to 2 mg/ml (Abs 0.1% = 0.512). The protein was then left for one week at 37° C under agitation at 250 rpm. Fibrils were isolated by centrifugation at 10.600 g for 15 minutes. The total amount of fibrils formed was determined using a Jasco V-650 spectrophotometer by the difference between the total amount of protein in solution before incubation and the total amount of protein left in solution in the supernatant at the end of the incubation period. The pellet was then suspended at a concentration of 1 mg/ml in sterile PBS. A small aliquot was used to confirm the presence of genuine amyloid fibrils by Congo red staining. PFFs and soluble mouse α-syn were stored at – 80 ºC. On the day of the surgery, α-syn PFFs were thawed and sonicated two cycles of 6 seconds 50 % power (10 microns amplitude) using a probe sonicator (Soniprep 150, MSE). A new aliquot of sonicated α-syn PFF was prepared every day of surgery. During the surgical procedure, α-syn PFFs were kept at room temperature while recombinant mouse wild-type α-syn monomer used for controls was kept at 4 ºC.

- Study design

Eight-to 9-week-old male C57BL6/C3H F1 mice were purchased from Charles River. All procedures involving animals were carried out in accordance with the European Communities Council Directive (2010/63/UE) and Spanish legislation (RD53/2013) on animal experiments and with approval from the ethical committee on animal welfare for our institution (Órgano Encargado del Bienestar Animal del Centro de Investigación Biomédica de La Rioja, OEBA-CIBIR). All efforts were made to minimize suffering and pain of the animals. Sample size was calculated using an online programme

(http://powerandsamplesize.com/Calculators/Compare-k-Means/1-Way-ANOVA-Pairwise). All animals were randomly distributed to the cages by a technician of the animal facilities and before any procedure; the cages were randomized to each group by a person not involved in the study. All the experiments were blinded and the investigators responsible for data collection and analysis were blinded.

C57BL6/C3H F1 mice were deeply anesthetized with isoflurane and received two 2.5-µl injections of sonicated murine α-syn PFF (5 µg), α-syn monomer (5 µg) or PBS into the dorsal striatum (5 µl total; AP +0.2, ML -2.0, DV -3.4 and -2.6 from the skull) at a rate at 0.25 µl/min as previously described (Luk et al., 2012). Control animals were injected with an equal volume of sterile mouse α-syn monomer or PBS. After each injection, the needle was left in place for 5 min and then slowly withdrawn. Animals were monitored post-surgery and sacrificed at various time points 15, 30 and 90 days post injection (dpi) by overdose with isofluorane. For histological studies, brains were removed after transcardial perfusion while, for biochemical studies, brains were dissected and immediately frozen and stored at -80 ºC until used.

- Behavioral assessment

To evaluate neuromuscular strength and motor coordination, the wire hang test was performed before intrastriatal injection and prior to sacrifice. Each mouse was placed on a wire lid of a conventional housing cage. The lid was lightly agitated to encourage the animal to grip the bars and then was turned upside down. The latency of mice to fall off the wire grid was measured and averaged over two trials (15 min apart). Trials were stopped if the mouse remained on the lid for over 15 min.

- Serum collection

For blood sampling, mice destined to biochemical studies were deeply anesthetized with an overdose of inhaled isofluorane and bled by cardiac puncture. Blood samples were collected in EDTA-free vials, allowed to clot at room temperature for four hours and stored

at 4 ºC overnight. The samples were centrifuged at 1200 x g for 10 min to isolate serum and stored at -80 ºC until processing.

- Multiplex determination of cytokines levels in serum

Serum levels of TNF-α, IFN-γ, IL-4, IL-5, IL-6 and IL-12/p70 were simultaneously determined using a multiplex immunoassay (ProcartaPlex™ Multiplex Immunoassays, Invitrogen™) according to the manufacturer's instructions. The fluorescent signals were measured using a Luminex 100/200 reader (Luminex Corp., TX, USA) and were analyzed using a standard curve for each cytokine specified above, which were generated with a five-parameter logistic curve-fitting method. Cytokines that were below detection limit were assigned a value of zero in all analysis.

- Immunohistochemistry

Animals were transcardially perfused with PBS followed by 4 % paraformaldehyde in PBS. After carefully removing the brains from the skull, were post-fixed overnight in 4 % paraformaldehyde, cryoprotected in 30 % sucrose, rapidly frozen and stored at -80 °C until use. 30-µm-thick coronal sections were prepared using a cryostat. Slices were washed with PBS and were incubated with 3% hydrogen peroxidase in PBS to inactivate the endogenous peroxidase. The slices were washed in PBS and were incubated with a blocking solution (0.1 M PBS containing 5% NGS 0.04% Triton X-100) for 1 h. Slices were incubated 24/48 hour at 4ºC with the primary antibodies: anti-TH (Anti-Tyrosine Hydroxylase Antibody, clone 2/40/15, Chemicon®, Millipore, Cat# MAB5280, RRID: AB_2201526, dilution 1:2000), anti-alpha-synuclein (phospho S129) (Anti-Alpha-synuclein (phospho S129) antibody [MJF-R13 (8-8)], Abcam, Cat# ab168381, RRID: AB_2728613, dilution 1:5000), anti-alpha-synuclein filament antibody (MJFR-14-6-4-2, conformation-specific, Abcam, Cat#ab209538, RRID: AB_2714215, dilution 1:40.000), anti-Iba1 (Anti-Iba1, Wako, Cat# 019-19741, RRID: AB_839504, dilution 1:500), anti-MHCII (MHC Class II (I-A/I-E) Monoclonal Antibody, Thermo Fisher Scientific, Cat# 14-5321-82, RRID: AB_467561,

dilution 1:500), anti-GFAP (Anti-Glial Fibrillary Acidic Protein antibody produced in rabbit, Sigma, Cat# G9269, RRID: AB_477035, dilution 1:2000). Slices were washed three times with PBS and were then incubated with fluorescent or biotinylated secondary antibody of the appropriate species. All the samples were processed simultaneously to obtain similar staining intensities.

The total number of TH-positive SNpc neurons was assessed by stereology in regularly spaced 30 µm-thick sections spanning the entire SNpc using StereoInvestigator software (MBF Bioscience). Striatal optical density (OD) of TH immunostaining was used as an index of the density of striatal dopaminergic innervation. Briefly, six representative rostro-caudal sections (at three levels of the striatum, bregma coordinates AP: +1.3, +0.5 and -0.4) were examined for each animal and regions of interest in the striatum were delineated and pixel densities were estimated using ImageJ. Background staining was quantified by measurement of pixel intensities in the white matter and subtracted from striatal regions for normalization.

For assessment of pathologic α-syn aggregates in the SNpc, 4 coronal sections (240 µm intervals between sections) for each animal were double labelled using antibodies against phospho S129 α-syn and TH to quantify intra-DA neuron alpha-synuclein inclusions. Numbers of S129 phospho-synuclein inclusions were manually quantified at 20x magnification from every eighth section (1:8 series) throughout the rostrocaudal axis of the SNpc. The data represent the total number of aggregates per section. Numbers of α-syn aggregates in the cortex and striatum were manually counted in 2 images (1 image from each hemisphere) for each section, with 3 representative sections (bregma coordinates AP: +1.3, +0.5 and -0.4) for each animal.

For evaluation of astroglial and microglial cells, sections were stained with GFAP, MHC class II and Iba1 antibodies. Iba1 and MHC class II staining was used to examine microglia activation while GFAP staining was used as an indicator of astrogliosis. Numbers of Iba1 and MHCII positive cells, as defined by those with darkly-stained cell bodies, were manually

counted at 20x magnification using digital photomicrographs. Estimation of the percentage of immunostained area by Iba1, MHC class II and GFAP positive cells was carried out using the threshold method of the ImageJ software (NIH). For the analyses of the SNpc, 4 coronal sections (240 µm intervals between sections, 1:8 series) for each animal and for each glial marker were included, whereas for the analyses of glial cells in the striatum and cortex, we included 3 selected representative rostro-caudal sections (bregma coordinates AP: +1.3, +0.5 and -0.4) for each animal and for each marker. Two images were taken at the same brain area of interest (1 image from each hemisphere) for each section. The Iba1 images in the brain regions examined were also qualitatively analyzed by using a 4 point categorical rating scale developed by Colburn and colleagues (Colburn et al., 1997), which provide an evaluation of microgliosis based on morphological and immunoreactivity changes, in a blinded fashion. The rating criteria and representative examples of each score are included in supplementary table 1.

- Quantitative PCR

Total RNA was isolated from frozen midbrain and cortical tissue samples using the RNeasy kit (Qiagen) according to the manufacturer's protocol. Subsequently, reverse transcription (RT) was performed with qSCRIP Reverse Transcriptase kit (Primer Design, Southampton, England) as per manufacturer's instruction. Transcripts obtained from the reverse transcriptase reaction were analyzed for IL-1β, TNF-α, IL-6 and IL-4 quantification by quantitative real-time PCR. qPCR experiments were performed on a StepOneTM Real-Time PCR system (Applied Biosystems) using Precision qPCR Mastermix (Applied Biosystems). The expression of each gene of interest was normalized by subtracting the cycle threshold (C_t) of β-actin from the gene of interest C_t (ΔC_t). The $2^{-\Delta\Delta Ct}$ method was then used to convert ΔC_t values to mRNA fold changes relative to the control group at each time point. The primer sequences for mouse IL-1β (forward: 5'- TGCCACCTTTTGACAGTGAT-3'; reverse: 5' GCTCTTGTTGATGTGCTGCT-3'), TNF-α (forward: 5'-ACGGCATGGATCTCAAAGAC-3'; reverse: 5'- GTGGGTGAGGAGCACGTAGT-3'), IL-6

(forward: ATGGATGCTACCAAACTGGAT; reverse: TGAAGGACTCTGGCTTTGTCT) and IL-4 (forward: 5'- CCAAGGTGCTTCGCATATTT-3'; reverse: 5'-ATCGAAAAGCCCGAAAGAGT-3') were synthesized by Sigma and the sequence for mouse actin (HK-SY-mo-600 against murine actin) was synthesized by Primer Design.

- Statistics

Data are presented as mean values ± the standard error of the mean (SEM). Statistical analyses were carried out using R-commander software (version 2.2-1, R Core Team, 2013). Statistical comparisons between experimental groups at each time point were performed with the parametric two-tailed Student's t test or one-way ANOVA as indicated. When variables were non-normally distributed, statistical differences were analyzed by non-parametric Mann Whitney U test or Kruskal-Wallis followed by Dunns test. A probability level of 0.05 or less was considered to be statistically significant.

Results

- Neuroinflammation precedes accumulation of α-syn aggregates in the SNpc after α-syn PFF injection.

Thirty mice were injected in the striatum with α-syn PFF and were sacrificed at 15 (n=10), 30 (n=10) or 90 (n=10) dpi. We included as control groups at each time point (n=10) mice injected with α-syn monomer or vehicle (PBS). In agreement with previous studies (Luk et al., 2012; Tran et al., 2014), the injection of α-syn PFF in the striatum of normal mice resulted in the progressive accumulation of phosphorylated α-syn inclusions in the SNpc. At 15 dpi sparse α-syn inclusions were observed in the SNpc, these increased significantly peaking at 30 dpi ($p=0.0162$ in comparison to 15 dpi) before decreasing at 90 dpi (Fig 1a, b; Sup Fig 1a). These α-syn inclusions were exclusively ipsilateral to the injection site at the time points examined. Immunohistochemical analysis of midbrain sections stained with TH and alpha-synuclein filament antibodies demonstrated the presence of oligomeric species of α-synuclein in dopaminergic neurons in the ipsilateral SNpc of α-syn PFF injected mice at

15 dpi (Sup Fig 1b). Dopaminergic striatal innervation was only decreased in the posterior striatum after 90 dpi ($p<0.001$, Fig 1c, d) and the number of DA neurons in the SNpc after 90dpi was decreased by 15% compared to the contralateral after 90 dpi (not statistically significant, Fig 1e, f), leading to a significant impairment in the wire hanging test performance ($p=0,025$) (Sup Fig 1c). Intrastriatal injection of α-syn monomer did not result in the presence of α-syn aggregation or striatal dopaminergic denervation or loss of DA neurons in the SNpc (Sup Fig 2).

Coronal brain sections of PBS, α-syn monomer and α-syn PFF injected mice were examined immunohistochemically for the microglial (Iba1) and astroglial (GFAP) activation markers. Quantification of the number of Iba1 positive cells in the SNpc region of the ipsilateral side of the brain after intrastriatal α-syn PFF injection revealed a significant increase at 15 dpi ($p<0,05$), at 30 dpi (non-significant) and at 90 dpi ($p<0,01$; Fig 2a, b). The number of Iba-1 positive cells in the ipsilateral SNpc of α-syn monomer injected mice remained unaltered and similar to control mice over time (Fig 2a, b). As expected, no differences in Iba1 staining were observed in the contralateral SNpc between control, α-syn monomer and α-syn PFF injected mice at any time point examined (Sup Fig 3a, b). Morphological microglia alterations were detected at 15, 30 and 90 dpi (Fig 2a, insets in upper panel) in α-syn PFF injected mice, with microglia presenting a bushy appearance with swollen cell bodies and intensely stained, thickened and branched processes, characteristic of an activated phenotype. The qualitative analyses of microgliosis in the ipsilateral SNpc confirmed these changes in the microglial morphology. Whereas control mice displayed a low qualitative rating score over time (Fig 2c), α-syn PFF injected mice achieved a significant higher qualitative rating score at 15 and 90 dpi ($p<0,01$; Fig 2c) compared to control mice. Injection of α-syn monomer induced significant changes in the microglial morphology only at 15 dpi ($p<0,01$) and PBS injection did not result in any change in the number or morphology of microglial cells in the ipsilateral and contralateral SNpc (Fig 2a, b, c, Sup Fig 3a, b).

The increase in the number of Iba1-positive cells in the ipsilateral SNpc of α-syn PFF injected mice was confirmed by an increase in the area occupied by Iba1-positive cells at 15 and 30 dpi compared to control mice (15d: p<0,001; 30d: p<0,01; Sup Fig 3c). The change in the microglial morphology observed in α-syn monomer injected mice at 15 dpi was also confirmed by a mild increase in the area occupied by Iba1-positive cells at this time point (p<0,05 non-significant), whereas the area occupied by Iba-1 cells in the other time points was similar to control mice (Sup Fig 3c). In the control mice, the PBS injection did not significantly affect the area occupied by Iba1-positive cells in the ipsilateral SNpc over time (Sup Fig 3c) and no differences in Iba1 staining were observed in the contralateral SNpc between control, α-syn monomer and α-syn PFF injected mice at any time point examined (Sup Fig 3d).

We also quantified MHC class II immunoreactive microglia within the SNpc at 15, 30 and 90 dpi after PBS, α-syn monomer and α-syn PFF injection. An increase in the number of MHC class II positive microglial cells was observed in α-syn monomer and α-syn PFF injected mice 15 dpi compared to control mice (non-significant, Sup Fig 4a, b). However, although the number of microglial cells expressing MHC class II in α-syn PFF injected mice was decreased at 30 dpi, these cells remained significantly increased in α-syn monomer injected mice (p<0,05; Sup Fig 4a, b). No MHC class II positive microglial cells were observed at 90 dpi in mice from any experimental group (Sup Fig 4b) or in the contralateral SNpc at any time point (data not shown).

We investigated whether microglial activation in the ispilateral SNpc of α-syn PFF injected mice was also accompanied by astrocyte activation. Intrastriatal α-syn PFF injection resulted in an increase in the area occupied by GFAP-positive cells in the ipsilateral SNpc at 15 and 30 dpi in comparison with control PBS-injected mice at each time point (15 dpi: p<0,05; 30 dpi: non-significant; Fig 2d, e). The area occupied by GFAP-positive cells in the ipsilateral SNpc of α-syn monomer injected mice was similar to control mice at all time points examined (Fig 2d, e). In the contralateral SNpc no GFAP-positive cells were

observed in control or α-syn monomer or α-syn PFF injected mice over time (data not shown).

We evaluated the mRNA expression of several inflammatory cytokines, IL-1β, TNF-α, IL-6 and IL-4, by qPCR in the ipsilateral SNpc of control, α-syn monomer and α-syn PFF injected mice at the various time points after injection. Interestingly, intrastriatal injection of α-syn PFF induced an increase of IL-1β mRNA expression in the ipsilateral SNpc at all times examined (15 dpi: p=0,0159; 30 dpi: non-significant; 90dpi: p=0,0317; Fig 2f, Table 1) compared to corresponding control mice at each time point. The expression levels of TNF-α in the ipsilateral SNpc of PFF α-syn injected mice were increased at 90 dpi compared to control mice at this time point (p=0,0015). A similar profile as for TNF-α was observed for IL-6, although did not reach statistical significance (Fig 2f, Table 1). IL-4 expression levels were all similar to the control mice at each time point (Table 1). The expression levels of IL-1β, TNF-α, IL-6 and IL-4 remained unaltered in α-syn monomer injected mice at all time points examined (Sup Fig 5a).

- Striatal neuroinflammatory response correlates with dopaminergic denervation in the α-syn PFF mouse model

Striatal α-syn PFF injection resulted in a progressive accumulation of α-syn aggregates in the ipsilateral striatum at 30 and 90 dpi, with the greatest number of phosphorylated α-syn inclusions observed at 90 dpi time point (p=0,0091 compared to 30 dpi, Sup Fig 6a, b). α-syn aggregates were absent in α-syn monomer injected mice (data not shown). We examined the temporal neuroinflammatory response in the striatum of α-syn PFF and α-syn monomer injected mice. The ipsilateral striatum showed an increase in the number of Iba1 positive cells after 15 and 30 dpi for all α-syn monomer, α-syn PFF and PBS injections (Fig 3b). This was increased in comparison with the contralateral striatum for all experimental groups (Sup Fig 6c), consistent with changes due to the surgical procedure. This moderate microgliosis decreased with time in all experimental groups and no changes in Iba1 staining were observed 90 days after PBS, α-syn monomer or α-syn PFF injection compared to

contralateral striatum (Fig 3a, b, Sup Fig 6c). These results were confirmed by analyzing the area occupied by Iba1 positive cells (Sup Fig 6d, e). The qualitative analyses of microgliosis in the ipsilateral striatum of control, α-syn monomer and α-syn PFF injected mice did not revealed any significant difference between the experimental groups over time (Fig 3c). In the same way, microglial cells expressing MHC class II in the ipsilateral striatum were increased at early time points while decreased at 90 dpi, although no differences between the experimental groups were observed at any time point (Sup Fig 4c, d). We did not observe MHC class II positive microglial cells in the contralateral striatum of mice from any experimental group over time (data not shown).

A similar temporal pattern as described for microglia activation was observed in astroglia activation at early time points after striatal injection, with a marked increase in the area occupied by GFAP cells in the ipsilateral striatum at 15 dpi in PBS, α-syn monomer and α-syn PFF injected mice (Fig 3d), due to the surgical procedure. At 30 and 90 dpi, control and α-syn monomer mice showed further reduction in astroglia activation and no differences between ipsilateral and contralateral striatum were observed (contralateral data not shown). However, the area occupied by GFAP positive cells in the ipsilateral striatum of α-syn PFF injected mice remained significantly increased (90 dpi: p=0,0120, Fig 3d, e). This striatal astrogliosis observed at 30 and 90 dpi in α-syn PFF mice was accompanied by a significant increase in the expression levels of IL-1β compared to control mice at the same time point (30 dpi: p=0,0238; 90 dpi: p=0,0159, Fig 3f, Table 1). The expression levels of TNF-α and IL-6 also were increased at 90 dpi in α-syn PFF mice, although did not reach statistical significance. Injection of α-syn monomer did not result in changes in cytokine expression levels over time compared to control mice (Sup Fig 5b).

- α-syn aggregation does not directly drives neuroinflammation

To assess if inflammatory response is related to α-syn aggregation, we examined other areas distal to the injection site known to display moderate α-syn inclusions, such as somatosensory cortex (Luk et al., 2012; Sorretino et al., 2017). Accumulation of

phosphorylated α-syn inclusions were detected in the ipsilateral cortex at 30 and 90 days after intrastriatal α-syn PFF injection (Sup Fig 7a, b). Contralateral cortex developed scarce α-syn pathology 90 dpi and α-syn aggregates were absent in α-syn monomer injected mice (data not shown).

The number and the area occupied by iba1-positive cells in the ipsilateral cortex were similar between experimental groups (Fig 4a, b and Sup Fig 7d). As expected, we did not observe any difference in the number and in the area occupied by iba-1 positive cells in the contralateral cortex of control, α-syn monomer and α-syn PFF injected mice over time (Sup Fig 7c, e). The qualitative analysis of microgliosis did not revealed any difference in the morphology of microglial cells between the experimental groups over time (Fig 4c). Although any difference was observed between the experimental groups at any time point, at 15 dpi we observed a slight increase in the area occupied by Iba1 cells and in the score of microglial morphology in the three experimental groups compared to 90 dpi, due to the surgical procedure. Immunohistochemical analysis of MHCII did not reveal any change in microglial MHCII expression in the cortex of mice from all experimental groups over time (data not shown) and the cytokines levels were also unaltered in the ipsilateral cortex of α-syn PFF mice over time compared to control mice at each time point (Table 1).

As described for striatum, an increase was observed in astroglia activation at early time points after striatal injection, with an increase in the area occupied by GFAP cells in the ipsilateral cortex at 15 and 30 dpi in control, α-syn monomer and α-syn PFF injected mice (Fig 4d, e), due to the surgical procedure. At 90 dpi, mice from all experimental groups showed further reduction in astroglia activation (Fig 4d, e).

- Intrastriatal α-syn PFF injection induces an increase in the serum levels of IL-6

Since some studies have demonstrated altered circulating levels of a series of cytokines in the serum of PD patients (Dobbs et al., 1999; Reale et al., 2009), we investigated whether intrastriatal α-syn PFF injection induced changes in the serum levels of specific cytokines.

Therefore, using multiplex immunoassays the levels of TNF-α, IFN-γ, IL-4, IL-5, IL-6 and IL-12p70 were determined in the serum of α-syn PFF and PBS injected mice at the 3 time points. Supplementary table 2 summarizes the mean (± standard error of the mean) values of cytokines expressed in pg/mL.

Since serum levels of cytokines in control mice did not vary over time (data not shown), all time points for the PBS injected mice were combined for comparison to α-syn PFF injected mice. Intrastriatal α-syn PFF injection resulted in a 3-fold increase in the serum level of IL-6 at 15 dpi (p=0,016) compared to control mice, with serum levels of IL-6 decreased at 30 and 90 dpi (Sup Table 1). However, the levels of the other cytokines did not differ significantly from the control mice at any time point (Sup Table 1).

Discussion

It is well documented that there is a close correlation between neuroinflammation and PD pathogenesis (McGeer et al., 2008; Halliday et al., 2011; Wang et al., 2015). However, a key question relates to whether neuroinflammation contributes to dopaminergic degeneration or is merely a secondary consequence of neuronal loss. Accrued evidence points to neuroinflammation acting as an active player in the α-syn-induced neurodegeneration. Studies to date in vitro (Beraud et al., 2013; Hoffmann et al., 2016) and in other α-syn based models of PD (Yamada et al., 2004; Theodore et al., 2008; Gao et al., 2011; Sanchez-Guajardo et al., 2010; Fischer et al., 2016; Thakur et al., 2017), support the idea that intracellular α-syn accumulation in the SNpc induces glial activation and release of inflammatory mediators, which mediate the loss of DA neurons. However, the supraphysiological α-syn levels or the α-syn species differences (human α-syn expressed in rat or mouse) limit the interpretation of the results. Recently, Duffy et al. investigated the temporal relationship of neuroinflammation in the rat model of synucleinopathy following intrastriatal injection of α-syn PFF, but they did not assess the neuroinflammatory response before α-syn inclusion formation (Duffy et al., 2018). We consider this information very

relevant to give new insights in the involvement of neuroinflammation in the pathogenesis of PD.

To investigate the time-course of glial activation prior to and following α-syn aggregation we used the α-syn PFF intrastriatal injected mouse model developed by Luk et al. (2012), which recapitulates the key pathological features of PD. Our data confirmed that intrastriatal injection of α-syn PFF led to intra-neuronal phosphorylated α-syn inclusions, loss of striatal dopaminergic innervation, selective loss of SNpc DA neurons and impaired motor coordination. The posterior part of the striatum showed a greater susceptibility to degenerate as previously described in other animal models and PD patients (Brooks et al., 2004; Blesa et al., 2012). The three time points evaluated reflect different stages of PD progression and represent a model to investigate whether microglial/astrocytes activation contributes to or is a consequence of α-syn aggregation and neuronal loss. The interpretation of our results is a variation to the previously proposed cascade of events (Gao et al., 2011; Duffy et al., 2018) as we propose the neuroinflammatory responses precede α-syn accumulation. However prolonged α-syn aggregation in the striatum appeared to correlate with decreased dopaminergic innervation and increased astrocytosis.

The increase in the number and the morphological changes of Iba1-positive cells in the ipsilateral SNpc of α-syn PFF injected mice 15 dpi is indicative of an early inflammatory response prior to significant α-syn accumulation. Our results are supported by data in PD patients implanted into the striatum with embryonic DA neurons (Olanow et al., 2019), which described inflammation and microglial activation in graft deposits long before the accumulation of α-syn pathology in implanted dopamine neurons. Moreover, it has been demonstrated in vivo that microglial depletion suppresses alpha-synuclein aggregation in alpha-synuclein PFF mice treated previously with PLX3397, an inhibitor of colony stimulating factor 1 receptor demonstrated to specifically deplete microglia (Guo et al., 2020). These observations support the hypothesis that microglial activation contributes to the development of α-syn pathology.

It is well documented that α-syn oligomers can induce an inflammatory response (Wilms et al., 2009; Kim et al., 2013; Fischer et al., 2016). The presence of alpha-synuclein oligomers and protofibrils in dopaminergic neurons at 15 dpi may be possible. These observations could explain our result that microglia activation precedes α-syn aggregation. However, the lack of changes in the number or morphology of Iba1-positive cells in the ipsilateral cortex, a region shown to display moderate α-syn inclusions, contradicts this relationship between α-syn pathology and microglia activation. It could be possible that other factors as rate of inclusion formation, achievement of certain brain region-dependent threshold in the number of neurons with α-syn pathology, local environment or glia density are involved in determining the microglial activation. In addition, single-cell transcriptomic analysis of microglia from discrete brain regions have revealed specific region-dependent subtypes of microglia (Grabert et al., 2016; Masuda et al., 2019), which could response to α-syn pathology in a different way. Nevertheless, our results suggest that microglial cells are activated as an early event in SNpc by a yet unknown mechanism. Future studies will be needed to investigate the trigger for microglia activation in the SNpc.

On other hand, microglial cells continue to be significantly activated at 90 dpi. Different signals given in the late time points from neurons with α-syn pathology could be involved in the late glial response, as release of α-syn from neurons or changes in neurotransmitter release or in proteins involved in the neuron-glia crosstalk (Fields et al., 2002; Liu et al., 2016). This glial activation is accompanied by the release of inflammatory cytokines. The increase in the expression levels of IL-1β and TNF-α in the SNpc at late time-point is in agreement with previous studies in PD brains and animal models (Mogi et al., 1994; Sriram et al., 2002; Wahner et al., 2007; Koprich et al., 2008). These studies concluded that both cytokines are toxic for the dopaminergic neurons of the SNpc, participating in the mechanism of cell death.

The activation of astrocytes also plays an important role in neuroinflammation (Colombo and Farina, 2016). Our results are in agreement with several studies demonstrating

astrogliosis in PD patients and animal models of PD (Kohutnicka et al., 1998; Miklossy et al., 2006; Booth et al., 2017; Yun et al., 2018). It has been suggested that astrocytic activation is induced by factors released by activated microglia, such as IL-1β and IL-6 (Woiciechowsky et al., 2004; Lin et al., 2006; Liddelow et al., 2017). Consequently, the acute microglia activation and the early increase in the IL-1β and IL-6 nigral levels could mediate astrocyte activation in the α-syn PFF injected mice. This result suggests a possible participation of astrocytes in the early neuroinflammatory response. The role of astrogliosis in PD has recently gained support from a study showing the prevention of conversion of astrocyte to an A1 neurotoxic phenotype is neuroprotective in animal models of PD (Yun et al., 2018).

Within the striatum, we did not observe microglial activation, suggesting that microglia activation in the striatum is not associated with α-syn accumulation, as reported previously by Duffy et al. 2018. However, interestingly, a significant astrogliosis was observed 90 dpi accompanied by a significant increase in the expression levels of IL-1β and IL-6. It has been described that the degeneration of the striatal dopaminergic innervation is followed by astrogliosis and that striatal astrocytes engulf dopaminergic debris in PD mouse models (Morales et al., 2016; Morales et al., 2017). Nevertheless, it could be possible that astrocytes participate in the process of degeneration of striatal dopaminergic terminals.

The intrastriatal injection of α-syn monomer only resulted in changes in the morphology of microglial cells in the ipsilateral SNpc, accompanied by an increase in the number of microglia cells expressing MHC class II. A previous study showed that non-aggregated WT synthetic α-syn induces an acute inflammatory response in vitro and in vivo 24 hours following intranigral injection (Couch et al., 2011). Our results would suggest an early microglial response to extracellular monomeric α-syn, possibly involving the engulfment or clearing of extracellular α-syn released from DA neurons by microglial cells for antigenic presentation in the context of MHC class II. This is in accordance with previous studies

demonstrating that extracellular monomeric α-syn enhance microglial phagocytosis (Park et al., 2008).

On the other hand, immune activation in PD is not restricted to brain sites and changes in the peripheral blood levels of some cytokines, including IL-6, have been reported by several authors (Dobbs et al., 1999; Reale et al., 2009; Scalzo et al., 2010; Pereira et al., 2016), as we observed in the α-syn injected mice at early time points. In addition, our results agree with a very recent study that have demonstrated that α-syn pathology in the CNS is sufficient to induce monocyte dysregulation in the periphery of a transgenic mouse model of PD (Grozdanov et al., 2019). All these data highlight the potential relation of the peripheral deregulation in the cytokine network with the neuroinflamatory process in PD.

Conclusions

In conclusion, although detailed mechanisms remain to be defined, we provide in vivo evidence that neuroinflammatory response precedes α-syn inclusion formation and is restricted to nigrostriatal area of α-syn PFF injected mice. Fig 5 summarizes the time course of synucleinopathy, neuroinflammation and degeneration in the SNpc (left graph) and striatum (right graph) following intrastriatal α-syn PFF injection. Our data adds novel insights into the mechanisms responsible for the etiology of PD and further identifies potential pathway for therapeutic intervention.

List of abbreviations

CNS: Central Nervous System

CSF: Cerebrospinal fluid

DA: Dopamine

dpi: days post-injection

GFAP: glial fibrillary acidic protein

LB: Lewy bodies

OD: Optical densitometry

PET: Positron emission tomography

PD: Parkinson's disease

SEM: standard error of the mean

SNpc: Substantia nigra pars compacta

TH: Tyrosine hydroxylase

WT: Wild type

α-syn PFF: alpha-synuclein pre-formed fibrils

α-syn: alpha-synuclein

Declarations

Ethics approval and consent to participate: All procedures involving animals were carried out in accordance with the European Communities Council Directive (2010/63/UE) and Spanish legislation (RD53/2013) on animal experiments and with approval from the ethical committee on animal welfare for our institution (Órgano Encargado del Bienestar Animal del Centro de Investigación Biomédica de La Rioja, OEBA-CIBIR).

Consent for publication: Not applicable.

Availability of data and materials: The datasets used and/or analysed during the current study are available from the corresponding author on reasonable request.

Competing interests: The authors declare that they have no competing interests.

Funding: This study was funded by the Instituto de Salud Carlos III (ISCIII), Ministerio de Ciencia, Innovacion y Universidades (CP1500200). Co-funded by European Regional Development Fund (FEDER) "A way to make Europe".

Authors' contributions: M.I. and L.A.E. designed the study. L.A.E. performed qPCR for analysis of expression levels of cytokines. M.I. performed alpha-synuclein PFFs mouse experiments and immunohistochemical analysis. F.J.B. performed stereological analysis. G.V. synthetized and prepared alpha-synuclein PFFs. M.I., J.M.C. and L.A.E. wrote the manuscript. All authors contributed to the manuscript and its amendments.

Acknowledgements: Not applicable.

Submission declaration: The work has not been published elsewhere and is not under review with another journal. All authors have read and approved the manuscript.

References

Barcia, C., Ros, C.M., Annese, V., et al., 2011. IFN-*γ* signaling, with the synergistic contribution of TNF-*α*, mediates cell specific microglial and astroglial activation in experimental models of Parkinson's disease. Cell Death & Disease 2: e142. doi: 10.1038/cddis.2011.17

Bartels, A.L., Willemsen, A.T., Doorduin, J., de Vries, E.F., Dierckx, R.A., Leenders, K.L., 2010. [11^{C}]-PK11195 PET: quantification of neuroinflammation and a monitor of anti-inflammatory treatment in Parkinson's disease? Parkinsonism & Related Disorders 16: 57-59. doi: 10.1016/j.parkreldis.2009.05.005

Beraud, D., Hathaway, H.A., Trecki, J., et al., 2013. Microglial activation and antioxidant responses induced by the Parkinson's disease protein alpha-synuclein. Journal of Neuroimmune Pharmacology 8: 94-117. doi: 10.1007/s11481-012-9401-0

Blesa, J., Pifl, C., Sánchez-González, M.A., et al., 2012. The nigrostriatal system in the presymptomatic and symptomatic stages in the MPTP monkey model: a PET, histological and biochemical study. Neurobiology of disease 48: 79-91. doi: 10.1016/j.nbd.2012.05.018

Blum-Degen, D., Muller, T., Kuhn, W., Gerlach, M., Przuntek, H., Riederer, P., 1995 Interleukin-1 beta and interleukin-6 are elevated in the cerebrospinal fluid of Alzheimer's and de novo Parkinson's disease patients. Neuroscience Letters 202: 17-20.

Booth, D.E., Hirst, W.D., Wade-Martins, R., 2017. The role of astrocyte dysfunction in Parkinson's disease pathogenesis. Trends in Neuroscience 40: 358-370. doi: 10.1016/j.tins.2017.04.001

Brooks, D.J., 2004. Neuroimaging in Parkinson's Disease. NeuroRx 1: 243-254. doi: 10.1602/neurorx.1.2.243

Colburn, R.W., DeLeo, J.A., Rickman, A.J., Yeager, M.P., Kwon, P., Hickey, W.F., 1997 Dissociation of microglial activation and neuropathic pain behaviors following peripheral nerve injury in the rat. Journal of Neuroimmunology 79: 163-175.

Colombo, E., Farina, C., 2016. Astrocytes: Key regulators of neuroinflammation. Trends in Immunology 37: 608-620. doi: 10.1016/j.it.2016.06.006

Couch, Y., Alvarez-Erviti, L., Sibson, N.R., Wood, M.J., Anthony, D.C., 2011. The acute inflammatory response to intranigral α-synuclein differs significantly from intranigral lipopolysaccharide and is exacerbated by peripheral inflammation. Journal of neuroinflammation 8: 166. doi: 10.1186/1742-2094-8-166

De Lella-Ezcurra, A.L., Chertoff, M., Ferrari, C., Graciarena, M., Pitossi, F., 2010 Chronic expression of low levels of tumor necrosis factor-alpha in the substantia nigra elicits progressive neurodegeneration, delayed motor symptoms and microglia/ macrophage activation. Neurobiology of Disease 37: 630-640. doi: 10.1016/j.nbd.2009.11.018

Dick, F.D., 2012. Parkinson's disease and pesticide exposures. British Medical Bulletin, 79-80: 219-231. doi: 10.1093/bmb/ldl018

Dobbs, R.J., Charlett, A., Purkiss, A.G., Dobbs, S.M., Weller, C., Peterson, D.W., 1999 Association of circulating TNF-alpha and IL-6 with ageing and parkinsonism. Acta neurologica Scandinavica 100: 34-41.

Duffy, M.F., Collier, T.J., Patterson, J.R., et al., 2018. Lewy body-like alpha-synuclein inclusions trigger reactive microgliosis prior to nigral degeneration. Journal of Neuroinflammation 15: 129. doi: 10.1186/s12974-018-1202-9

Ebrahimi-Fakhari, D., Wahlster, L., McLean, P.J., 2012. Protein degradation pathways in Parkinson's disease – curse or blessing. Acta Neuropathology, 124: 153–172. doi: 10.1007/s00401-012-1004-6

Fearnley, J.M., Lees, A.J., 1991. Ageing and Parkinson's disease: substantia nigra regional selectivity. Brain, 114: 2283.

Ferrari, C.C., Pott Godoy, M.C., Tarelli, R., Chertoff, M., Depino, A.M., Pitossi, F.J., 2006. Progressive neurodegeneration and motor disabilities induced by chronic expression of IL-1beta in the substantia nigra. Neurobiology of Disease 24: 183–193. doi: 10.1016/j.nbd.2006.06.013

Fields, R.D. and Stevens-Graham, B., 2002. New Insights into Neuron-Glia Communication. Science 298: 556-562. doi: 10.1126/science.298.5593.556

Fischer, D.L., Gombash, S.E., Kemp, C.J., et al., 2016. Viral Vector-Based Modeling of Neurodegenerative Disorders: Parkinson's Disease. Methods in molecular biology 1382: 367-382. doi: 10.1007/978-1-4939-3271-9_26

Gagne, J.J., Power, M.C., 2010. Anti-inflammatory drugs and risk of Parkinson disease: a meta-analysis. Neurology 74: 995-1002. doi: 10.1212/WNL.0b013e3181d5a4a3

Gao, H.M., Zhang, F., Zhou, H., et al., 2011. Neuroinflammation and α-Synuclein Dysfunction Potentiate Each Other, Driving Chronic Progression of Neurodegeneration in a Mouse Model of Parkinson's Disease. Environmental Health Perspectives 119: 807-814. doi: 10.1289/ehp.1003013

Gerhard, A., Pavese, N., Hotton, G., et al., 2006. In vivo imaging of microglial activation with [11C](R)-PK11195 PET in idiopathic Parkinson's disease. Neurobiology of Disease 21: 404–412. doi: 10.1016/j.nbd.2005.08.002

Grabert, K., Michoel, T., Karavolos, M.H., et al., 2016. Microglial brain region-dependent diversity and selective regional sensitivities to aging. Nature neuroscience 19: 504-16. Doi: 10.1038/nn.4222

Greenamyre, J.T., Hastings, T.G., 2004. Biomedicine. Parkinson's–divergent causes, convergent mechanisms. Science 304: 1120–1122. doi: 10.1126/science.1098966

Grozdanov, V., Bousset, L., Hoffmeister, M., et al., 2019. Increased immune activation by pathologic alpha-synuclein in Parkinson's Disease. Annals of neurology epub ahead of print. doi: 10.1002/ana.25557

Halliday, G.M., Stevens, C.H., 2011. Glia: initiators and progressors of pathology in Parkinson's disease. Movement Disorders 26: 6–17. doi: 10.1002/mds.23455

Hamza, T.H., Zabetian, C.P., Tenesa, A., et al., 2010. Common genetic variation in the HLA region is associated with late-onset sporadic Parkinson's disease. Nature Genetics 42: 781–785. doi: 10.1038/ng.642

Hoffmann, A., Ettle, B., Bruno, A., 2016. Alpha-synuclein activates BV2 microglia dependent on its aggregation state. Biochemical and Biophysical Research Communications 479: 881-886. doi: 10.1016/j.bbrc.2016.09.109

Kim, C., Ho, D.H., Suk, J.E., et al., 2013. Neuron-released oligomeric α-synuclein is an endogenous agonist of TLR2 for paracrine activation of microglia. Nature Communications 4: 1562. doi: 10.1038/ncomms2534

Kohutnicka, M., Lewandowska, E., Kurkowska-Jastrzebska, I., Członkowski, A., 1998. Microglial and astrocytic involvement in a murine model of Parkinson's disease induced by 1-methyl-4-phenyl-1,2,3,6-tetrahydropyridine (MPTP). Immunopharmacology 39:167-180.

Koprich, J.B., Reske-Nielsen, C., Mithal, P., Isacson, O., 2008. Neuroinflammation mediated by IL-1β increases susceptibility of dopamine neurons to degeneration in an animal model of Parkinson's disease. Journal of Neuroinflammation 5: 8. doi: 10.1186/1742-2094-5-8

Lee, H.J., Suk, J.E., Patrick, C., et al., 2010. Direct transfer of α-synuclein from neuron to astroglia causes inflammatory responses in synucleinopathies. The Journal of biological chemistry 285: 9262–9272. doi: 10.1074/jbc.M109.081125

Liddelow, S.A., Guttenplan, K.A., Clarke, L.E., et al., 2017. Neurotoxic reactive astrocytes are induced by activated microglia. Nature 541: 481-487. doi: 10.1038/nature21029

Lin, M.T., Beal, M.F., 2006. Mitochondrial dysfunction and oxidative stress in neurodegenerative diseases. Nature 443: 787–795. doi: 10.1038/nature05292

Lin, H.W., Basu, A., Druckman, C., Cicchese, M., Krady, J.K., Levison, S.W., 2006. Astrogliosis is delayed in type 1 interleukin-1 receptor-null mice following a penetrating brain injury. Journal of Neuroinflammation, *3*, 15. doi: 10.1186/1742-2094-3-15

Lindqvist, D., Hall, S., Surova, Y., et al., 2013. Cerebrospinal fluid inflammatory markers in Parkinson's disease: associations with depression, fatigue, and cognitive impairment. Brain, Behaviour and Immunity 33: 183–189. doi: 10.1016/j.bbi.2013.07.007

Liu, H., Leak, R.K., Hu, X., 2016. Neurotransmitter receptors on microglia. Stroke Vasc Neurol 1: 52-58. doi: 10.1136/svn-2016-000012

Long-Smith, C.M., Sullivan, A.M., Nolan, Y.M., 2009. The influence of microglia on the pathogenesis of Parkinson's disease. Progress in Neurobiology; 89: 277–287. doi: 10.1016/j.pneurobio.2009.08.001

Luk, K.C., Kehm, V., Carroll, J., et al., 2012. Pathological α-alpha-synuclein transmission initiates Parkinson-like neurodegeneration in nontransgenic mice. Science 338: 949-953. doi: 10.1126/science.1227157

Manthripragada, A.D., Schernhammer, E.S., Qiu, J., et al., 2011. Non-steroidal anti-inflammatory drug use and the risk of Parkinson's disease. Neuroepidemiology 36: 155-161. doi: 10.1159/000325653

Masuda, T., Sankowski, R., Staszewski, O., et al., 2019. Spatial and temporal heterogeneity of mouse and human microglia at single-cell resolution. Nature 566: 388-392. Doi: 10.1038/s41586-019-0924-x

McGeer, P.L., Itagaki, S., Boyes, B.E., McGeer, E.G., 1988. Reactive microglia are positive for HLA-DR in the substantia nigra of Parkinson's and Alzheimer's disease brains.

Neurology 38: 1285–1291.

McGeer, P.L., McGeer, E.G., 2008. Glial reactions in Parkinson's disease. Movement Disorders 23: 474-483. doi: 10.1002/mds.21751

Miklossy, J., Doudet, D.D., Schwab, C., Yu, S., McGeer, E.G., McGeer, P.L., 2006. Role of ICAM-1 in persisting inflammation in Parkinson disease and MPTP monkeys. Experimental Neurology 197: 275-283. doi: 10.1016/j.expneurol.2005.10.034

Mogi, M., Harada, M., Kondo, T., et al., 1994. Interleukin-1β, interleukin-6, epidermal growth factor and transforming growth factor-α are elevated in the brain from parkinsonian patients. Neuroscience Letters 180: 147–150.

Morales, I., Sanchez, A., Rodriguez-Sabate, C., Rodriguez, M., 2016. The astrocytic response to the dopaminergic denervation of the striatum. Journal of Neurochemistry 139: 81-95. doi: 10.1111/jnc.13684

Morales, I., Sanchez, A., Rodriguez-Sabate, C., Rodriguez, M., 2017. Striatal astrocytes engulf dopaminergic debris in Parkinson's disease: A study in an animal model. Plos One 12: e0185989. doi: 10.1371/journal.pone.0185989

Olanow, C.W., Kieburtz, K., Katz, R., 2017. Clinical approaches to the development of a neuroprotective therapy for PD. Experimental Neurology 298: 246-251. doi: 10.1016/j.expneurol.2017.06.018

Olanow, C.W., Savolainen, M., Chu, Y., Halliday, G.M., Kordower, J.H., 2019. Temporal evolution of microglia and α-synuclein accumulation following foetal grafting in Parkinson's disease. Brain 142: 1690-1700. doi: 10.1093/brain/awz104

Park, J.Y., Paik, S.R., Jou, I., Park, S.M., 2008. Microglial phagocytosis is enhanced by monomeric alpha-synuclein, not aggregated alpha-synuclein: implications for Parkinson's disease. Glia 56: 1215-1223. doi: 10.1002/glia.20691

Pereira, J.R., Santos, L.V.D., Santos, R.M.S., et al., 2016. IL-6 serum levels are elevated in Parkinson's disease patients with fatigue compared to patients without fatigue. Journal of the neurological sciences 370: 153-156. doi: 10.1016/j.jns.2016.09.030

Reale, M., Larlori, C., Thomas, A., et al., 2009. Peripheral cytokines profile in Parkinson's disease. Brain, behavior and immunity 23: 55-63. doi: 10.1016/j.bbi.2008.07.003

Sanchez-Guajardo, V., Febbraro, F., Kirik, D., Romero-Ramos, M., 2010. Microglia acquire distinct activation profiles depending on the degree of alpha-synuclein neuropathology in a rAAV based model of Parkinson's disease. Plos one 5: e8784. doi: 10.1371/journal.pone.0008784

Scalzo, P., Kümmer, A., Cardoso, F., Teixeira, A.L., 2010. Serum levels of interleukin-6 are elevated in patients with Parkinson's disease and correlate with physical performance. Neuroscience letters 468: 56-58. doi: 10.1016/j.neulet.2009.10.062

Schapira, A.H., 2006. Mitochondrial disease. Lancet 368: 70–82. doi: 10.1016/S0140-6736(06)68970-8

Sorrentino, Z.A., Brooks, M.M.T., Hudson, V., et al., 2017. Intrastriatal injection of α-synuclein can lead to widespread synucleinopathy independent of neuroanatomic connectivity. Molecular Neurodegeneration 12: 40. doi: 10.1186/s13024-017-0182-z

Sriram, K., Matheson, J.M., Benkovic, S.A., Miller, D.B., Luster, M.I., O'Callaghan, J.P., 2002. Mice deficient in TNF receptors are protected against dopaminergic neurotoxicity:

implications for Parkinson's disease. Faseb Journal 16: 1474-1476. doi: 10.1096/fj.02-0216fje

Thakur, P., Breger, L.S., Lundblad, M., et al., 2017. Modeling Parkinson's disease pathology by combination of fibril seeds and α-synuclein overexpression in the rat brain. Proc Natl Acad Sci USA 114: e8284e8293. doi: 10.1073/pnas.1710442114

Theodore, S., Cao, S., McLean, P.J., Standaert, D.G., 2008. Targeted overexpression of human alpha-synuclein triggers microglial activation and an adaptive immune response in a mouse model of Parkinson's disease. Journal of Neuropathology & Experimental Neurology 67: 1149-1158. doi: 10.1097/NEN.0b013e31818e5e99

Tran, H.T., Chung, C.H., Iba, M., et al., 2014. Alpha-synuclein immunotherapy blocks uptake and templated propagation of misfolded α-alpha-synuclein and neurodegeneration. Cell Reports 7: 2054-2065. doi: 10.1016/j.celrep.2014.05.033

Wahner, A.D., Sinsheimer, J.S., Bronstein, J.M., Ritz, B., 2007. Inflammatory cytokine gene polymorphisms and increased risk of Parkinson disease. Archives of neurology 64: 836-840. doi: 10.1001/archneur.64.6.836

Wang, Q., Liu, Y., Zhou, J., 2015. Neuroinflammation in Parkinson's disease and its potential as therapeutic target. Translational neurodegeneration 4: 19. doi: 10.1186/s40035-015-0042-0

Wilms, H., Rosenstiel, P., Romero-Ramos, M., et al., 2009. Suppression of MAP kinases inhibits microglial activation and attenuates neuronal cell death induced by alpha-synuclein protofibrils. International Journal of Immunopathology and pharmacology 22: 897-909. doi: 10.1177/039463200902200405

Woiciechowsky, C., Stoltenburg-Didinger, G., Stockhammer, F., Volk, H.D., 2004. Brain-IL-1 beta triggers astrogliosis through induction of IL-6: inhibition by propranolol and IL-10. Medical science monitor 10: 325-330.

Yamada, T., Kawamata, T., Walker, D.G., McGeer, P.L., 1992. Vimentin immunoreactivity in normal and pathological human brain tissue. Acta Neuropathologica 84: 157–162.

Yamada, M., Iwatsubo, T., Mizuno, Y., Mochizuki, H., 2004. Overexpression of alpha-synuclein in rat substantia nigra results in loss of dopaminergic neurons, phosphorylation of alpha-synuclein and activation of caspase-9: resemblance to pathogenetic changes in Parkinson's disease. Journal of neurochemistry 91: 451-61. doi: 10.1111/j.1471-4159.2004.02728.x

Yun, S.P., Kam, T.I., Panicker, N., et al., 2018. Block of A1 astrocyte conversion by microglia is neuroprotective in models of Parkinson's disease. Nature Medicine 24: 931-938. doi: 10.1038/s41591-018-0051-5

Figure captions

Figure 1: Analysis of α-syn aggregation and DA neurons in SNpc and striatal dopaminergic innervation in the α-syn PFF mouse model. a) Representative images of intraneuronal phospho-α-syn inclusions in the ipsilateral SNpc of α-syn PFF and PBS (Control) injected mice at various dpi. Scale bars represent 200 µm (top panels) and 50 µm (low panels) b) Quantification of Ser129 phospho-α-syn positive aggregates in the ipsilateral SNpc at 15, 30 and 90 dpi. Data are expressed as mean ± SEM (n=4-8). *p<0,01 different from PFF 15d, non-parametric Mann Whitney U test. c) Photomicrographs of striatal sections showing TH immunolabeling of mice at 15, 30 and 90 dpi or at 90 dpi after control (PBS) injection. d) Optical density quantification of ipsilateral striatal TH normalized to the contralateral striatum. Data are expressed as mean ± SEM (n=4-8). ***p<0,001 compared to Control group, parametric Student's t-test. e) TH staining of dopaminergic neurons in a coronal section of the midbrain in α-syn PFF and Control injected mice at increasing dpi. Scale bar represents 500 µm. Arrow points to the decrease in the number of DA neurons. f) Unbiased stereologic quantification of TH-immunoreactive neurons in ipsilateral and contralateral SNpc of mice injected with α-syn PFF or Control (PBS) at increasing dpi. Data are expressed as mean ± SEM (n=4-8).

Figure 2: Glial cell activation in the SNpc of α-syn PFF injected mice. a) Representative images of ipsilateral SNpc sections immunolabeled with Iba1 microglial marker from Control (PBS), α-syn monomer and α-syn PFF injected mice at increasing dpi. Scale bar represents 50 µm. Insets show images at higher magnification (scale bar 10 µm). b) Quantification of the number of Iba1-positive cells in the ipsilateral SNpc of Control (PBS), α-syn monomer and α-syn PFF injected mice with increasing dpi. Data are expressed as mean ± SEM (n= 4-8). *p<0,05, **p<0,01 compared to control at same time point, ΔΔp<0,01 compared to Monomer, one-way ANOVA. c) Qualitative rating of microgliosis in the ipsilateral SNpc revealed by Iba1 immunohistochemistry using a 4 point scale ranging from 0 (no microgliosis) to 3 (pronounced microgliosis) according to microglia

morphology. Values are expressed as mean ± SEM (n= 4-8). **p<0,01 compared to control, Δp<0,05 compared to Monomer, one-way ANOVA. d) Representative images of ipsilateral SNpc double immunostained against TH (in red) and GFAP (in green) of Control (PBS), α-syn monomer and α-syn PFF injected mice. Scale bars: 40 µm. e) Analysis of the area occupied by GFAP-positive cells in the ipsilateral SNpc of control, α-syn monomer and α-syn PFF injected mice. Data are expressed as mean ± SEM (n= 4-8). *p<0,05 compared to control, Δp<0,05 compared to Monomer, one-way ANOVA. f) Fold changes in IL-1β, TNF-α and IL-6 mRNA levels in the ipsilateral midbrain of α-syn PFF injected mice at 15, 30 and 90 dpi. Fold changes were relative to the control group at each time point. The control group value at each time point is set at 1.0 as indicated by the dashed line. Data are expressed as mean ± SEM (n=4). Non-parametric Mann Whitney U test, statistical analyses compared to control group at each time point, *p<0.05, **p<0,01.

Figure 3: Neuroinflammatory response in the striatum. a) Representative images of ipsilateral striatal sections immunolabeled with Iba1 microglial marker in control, α-syn monomer and α-syn PFF injected mice at 90 dpi. Scale bar represents 50 µm. b) Quantification of the number of Iba1-positive cells in the ipsilateral striatum of Control (PBS), α-syn monomer and α-syn PFF injected mice. Data are expressed as mean ± SEM (n= 4-8). c) Qualitative rating of ipsilateral striatal microgliosis revealed by Iba1 immunohistochemistry using a 4 point scale ranging from 0 (no microgliosis) to 3 (pronounced microgliosis) according to microglia morphology. Data are expressed as mean ± SEM (n= 4-8). d) Analysis of the area occupied by GFAP positive cells in the ipsilateral striatum of Control (PBS), α-syn monomer and α-syn PFF injected mice with increasing dpi. Data are expressed as mean ± SEM (n= 4-8). *p<0,05 compared to control, one-way ANOVA. e) Representative images of ipsilateral striatum immunostained against GFAP (green) of Control (PBS), α-syn monomer and α-syn PFF injected mice at 90 dpi. Scale bar represents 50 µm. f) Fold changes in IL-1β, TNF-α and IL-6 mRNA levels in the ipsilateral striatum of α-syn PFF injected mice at 15, 30 and 90 dpi. Fold changes were relative to the

control group at each time point. The control group value at each time point is set at 1.0 as indicated by the dashed line. Data are expressed as mean ± SEM (n=4-8). Non-parametric Mann Whitney U test, statistical analyses compared to control group at each time point, *p<0.05.

Figure 4: Analysis of glial cell activation in the cortex. a) Representative images of ipsilateral cortical sections immunolabeled with Iba1 microglial marker in Control (PBS), α-syn monomer and α-syn PFF injected mice 15, 30 and 90 dpi. Scale bar represents 50 µm. Insets show images at higher magnification (scale bar 10 µm). b) Quantification of the number of Iba1-positive cells in the ipsilateral cortex of Control (PBS), α-syn monomer and α-syn PFF injected mice. c) Qualitative rating of ipsilateral cortical microgliosis revealed by Iba1 immunohistochemistry using a 4 point scale ranging from 0 (no microgliosis) to 3 (pronounced microgliosis) according to microglia morphology. d) Quantified percentage of area occupied by GFAP-positive cells in the ipsilateral cortex of Control (PBS), α-syn monomer and α-syn PFF injected mice. e) Representative images of ipsilateral cortical sections labeled for GFAP immunoreactive astroglia from control, α-syn monomer and α-syn PFF injected mice. Scale bar represents 40 µm. Data are expressed as mean ± SEM (n=4-8). One-way ANOVA, statistical analyses compared to control group at each time point.

Figure 5: Time course of α-syn aggregation, neuroinflammation and neurodegeneration in the nigrostriatal area of the α-syn PFF mouse model. The figure summarizes the main temporal changes that occur in the SNpc (left graph) and striatum (right graph) following striatal α-syn PFF injection. Data represent the percentage of change relative to control at each time point.

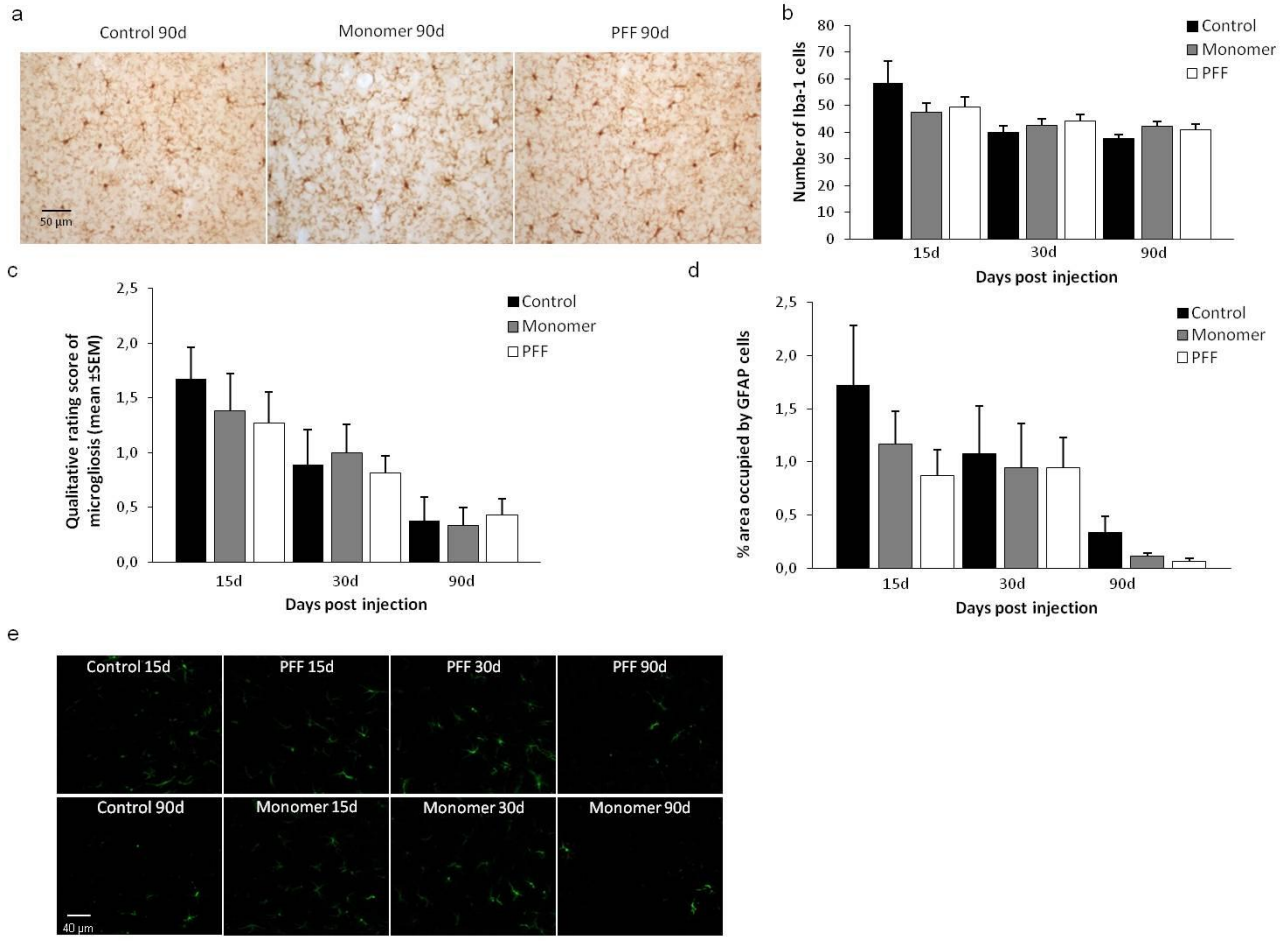
a
Control 90d
Monomer 90d
PFF 90d
50 µm
b
Number of Iba-1 cells
Control
Monomer
PFF
Days post injection
c
Qualitative rating score of microgliosis (mean ±SEM)
Control
Monomer
PFF
Days post injection
d
% area occupied by GFAP cells
Control
Monomer
PFF
Days post injection
e
Control 15d
PFF 15d
PFF 30d
PFF 90d
Control 90d
Monomer 15d
Monomer 30d
Monomer 90d
40 µm

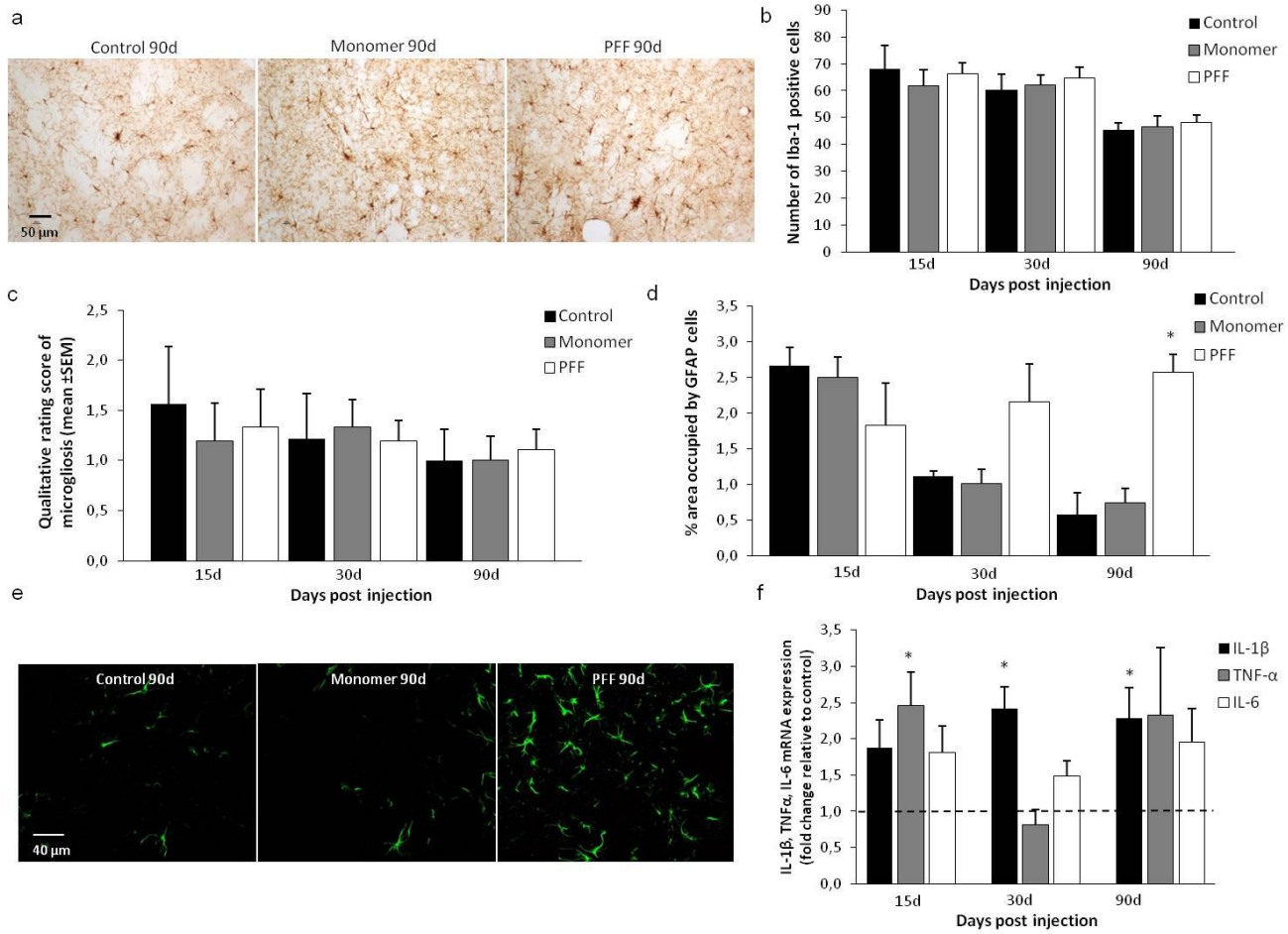
a
Control 90d
Monomer 90d
PFF 90d
50 µm
b
Number of Iba-1 positive cells
Control
Monomer
PFF
15d
30d
90d
Days post injection
c
Qualitative rating score of microgliosis (mean ±SEM)
Control
Monomer
PFF
15d
30d
90d
Days post injection
d
% area occupied by GFAP cells
Control
Monomer
PFF
15d
30d
90d
Days post injection
e
Control 90d
Monomer 90d
PFF 90d
40 µm
f
IL-1β, TNFα, IL-6 mRNA expression (fold change relative to control)
IL-1β
TNF-α
IL-6
15d
30d
90d
Days post injection

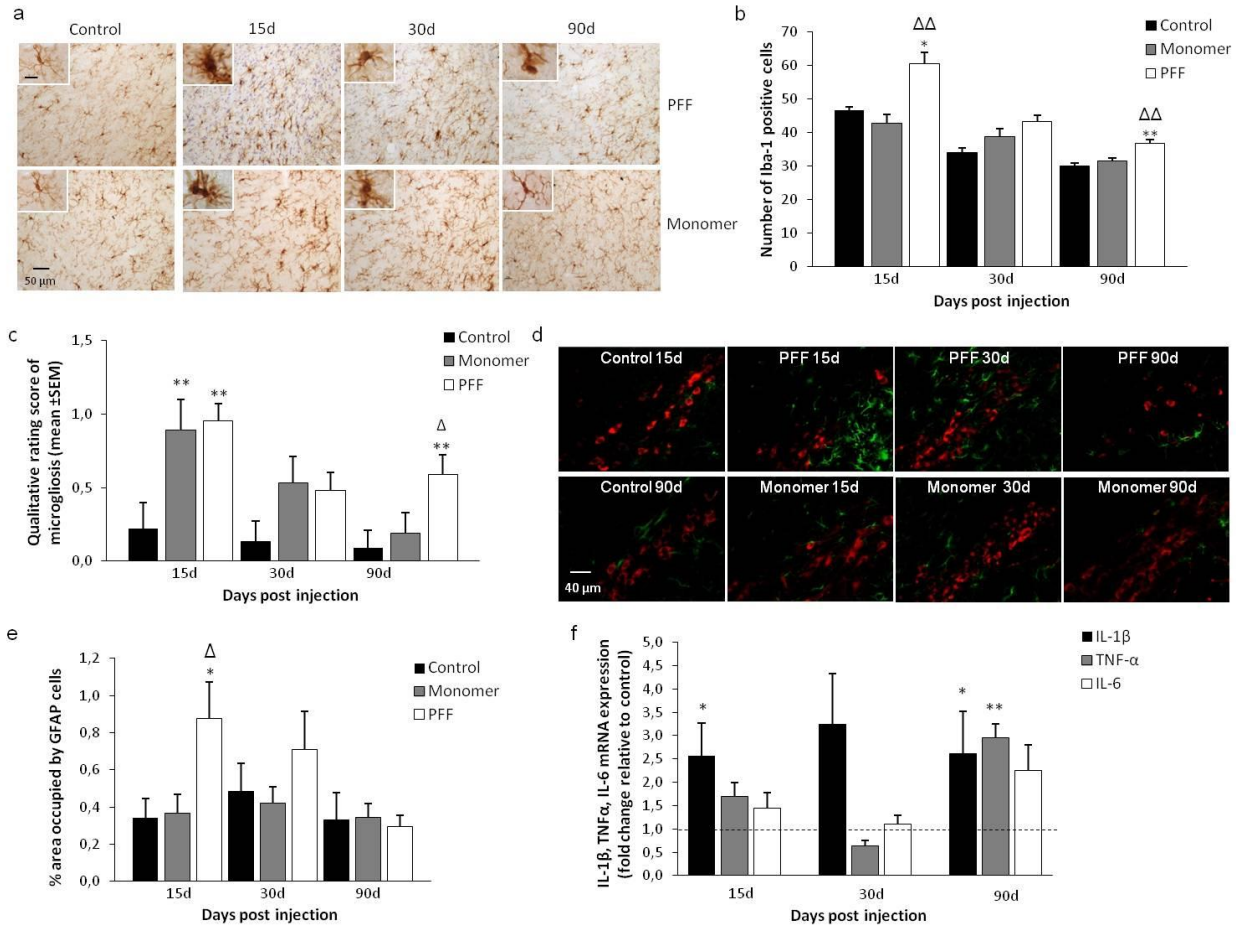
a
Control
15d
30d
90d
PFF
Monomer
50 µm
b
Number of Iba-1 positive cells
Control
Monomer
PFF
15d
30d
90d
Days post injection
c
Qualitative rating score of microgliosis (mean ±SEM)
Control
Monomer
PFF
15d
30d
90d
Days post injection
d
Control 15d
PFF 15d
PFF 30d
PFF 90d
Control 90d
Monomer 15d
Monomer 30d
Monomer 90d
40 µm
e
% area occupied by GFAP cells
Control
Monomer
PFF
15d
30d
90d
Days post injection
f
IL-1β, TNFα, IL-6 mRNA expression (fold change relative to control)
IL-1β
TNF-α
IL-6
15d
30d
90d
Days post injection

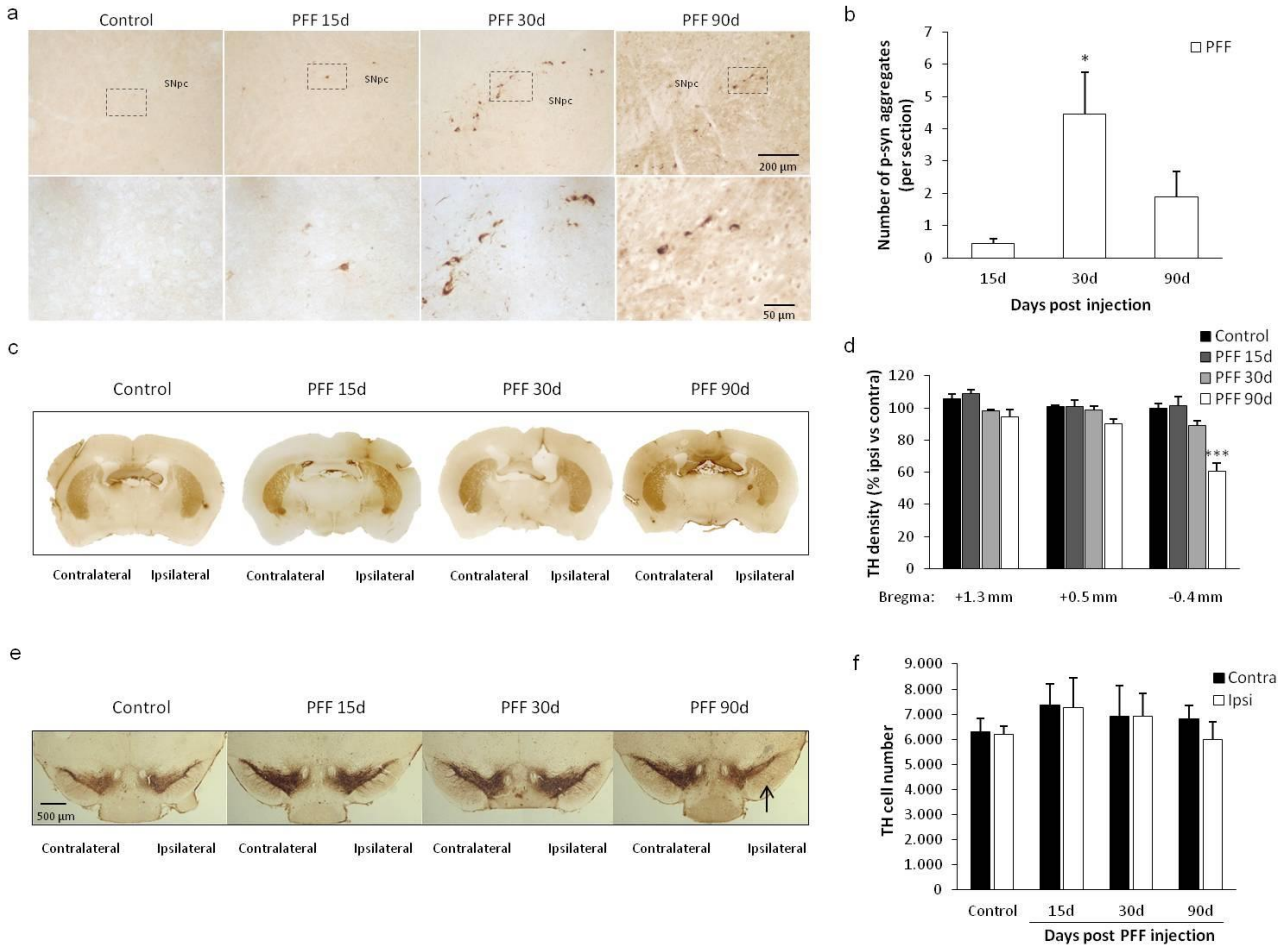
a
Control
PFF 15d
PFF 30d
PFF 90d
SNpc
200 µm
50 µm
b
PFF
Number of p-syn aggregates (per section)
Days post injection
15d
30d
90d
c
Control
PFF 15d
PFF 30d
PFF 90d
Contralateral
Ipsilateral
d
Control
PFF 15d
PFF 30d
PFF 90d
TH density (% ipsi vs contra)
Bregma:
+1.3 mm
+0.5 mm
-0.4 mm
e
500 µm
f
Contra
Ipsi
TH cell number
Control
15d
30d
90d
Days post PFF injection

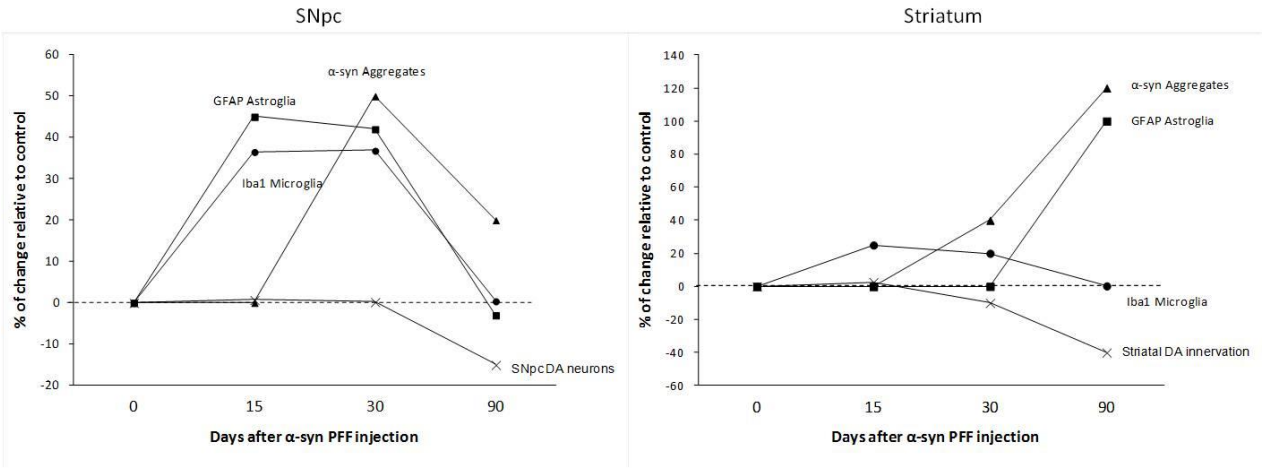

Table 1: qRT-PCR analysis for mRNA levels of cytokines in ipsilateral midbrain, cortex and striatum of control and α-syn PFF mice over time. The results are expressed as average fold change relative to the controls ± SEM, n=5 in each group. Non-parametric Kruskal-Wallis test, statistical analyses compared to control group, *p<0.05, **p<0,01.

	Experimental group			
Cytokine (Fold mRNA)	**Control**	**PFF 15d**	**PFF 30d**	**PFF 90d**
Midbrain				
IL-1β	1,00 ± 0,20	2,57 ± 0,70 *	2,59 ± 0,10	2,62 ± 0,91 *
IL-6	1,00 ± 0,15	1,44 ± 0,33	1,10 ± 0,19	2,25 ± 0,56
TNF-α	1,00 ± 0,33	1,86 ± 0,44	0,69 ± 0,11	2,44 ± 0,61**
IL-4	1,00 ± 0,20	0,90 ± 0,17	0,87 ± 0,13	0,82 ± 0,12
Striatum				
IL-1β	1,00 ± 0,20	1,88 ± 0,38	3,21 ± 0,82 *	3,17 ± 0,94*
IL-6	1,00 ± 0,19	1,81 ± 0,37	1,48 ± 0,21	1,96 ± 0,46
TNF-α	1,00 ± 0,14	2,92 ± 0,52 *	0,81 ± 0,21	2,33 ± 0,93
IL-4	1,00 ± 0,27	1,48 ± 0,35	0,64 ± 0,17	1,72 ± 0,63
Cortex				
IL-1β	1,00 ± 0,12	1,31 ± 0,36	1,71 ± 0,19	1,87 ± 0,29
IL-6	1,00 ± 0,16	1,18 ± 0,34	1,35 ± 0,21	1,53 ± 0,22
TNF-α	1,00 ± 0,28	1,15 ± 0,17	1,28 ± 0,08	1,44 ± 0,18
IL-4	1,00 ± 0,18	1,16 ± 0,16	1,42 ± 0,30	1,63 ± 0,21